DNA / protein binding and magnetic property studies of 1D Cu(II) complex containing fumarate and tridentate Schiff base ligands

Aparup Paul,[a] Valerio Bertolasi,[b] Albert Figuerola,[c] Subal Chandra Manna[a]

[a] *Department of Chemistry and Chemical Technology, Vidyasagar University, Midnapore 721102, West Bengal, India, E-mail: scmanna@mail.vidyasagar.ac.in, Fax: (91) (03222) 275329.*

[b]*Dipartimento di Scienze Chimiche e Farmaceutiche, Centro di Strutturistica Diffrattometrica, Università di Ferrara, Via L. Borsari, 46, 44100 Ferrara, Italy.*

[c] *Departament de Química Inorgànica i Orgànica (Secció de Química Inorgànica) and Institut de Nanociència i Nanotecnologia (IN2UB), Universitat de Barcelona , Martí i Franquès 1-11, 08028 Barcelona, Spain.*

ID copper(II) complex, $[Cu_2(L)_2(fum)]\cdot H_2O\}_n$ (**1**) has been synthesized using fumarate (fum^{2-}) and a Schiff base (HL), derived from the condensation reaction of 2-amino-1-butanol and salicyldehyde. Complex **1** has been characterized by X-ray crystal structure, FT-IR, electronic absorption and fluorescence spectroscopic methods. The structural determination reveals that complex **1** crystallizes in the monoclinic system with space group P21/n and form 1D polymeric chain, built by bridging fum. Weak $\pi\ldots\pi$ and C–H$\ldots\pi$ interactions in **1**, lead to a 3D supramolecular architecture. Complex **1** exhibits fluorescence at room temperature with a quantum yield (Φ_s) of 0.257. The interactions of complex **1** with bovine serum albumin (BSA) and human serum albumin (HSA) were studied using electronic absorption and fluorescence spectroscopic techniques and the analysis shows that complex **1** interaction with BSA / HSA occurs mainly with ground state association process. Calculated values of apparent association constants are 1.34×10^4 M^{-1} and 1.81×10^4 M^{-1} for BSA and HAS, respectively, at 300 K. The number of binding sites and binding constants were calculated using double logarithm regression equation. The

interaction of complex **1** with the calf thymus DNA (CT-DNA) was also investigated using electronic absorption and fluorescence spectroscopic methods. The results show that complex **1** has binding affinity to CT-DNA in the order of 2.96×10^5 M^{-1}. Low temperature magnetic measurements reveal existence of antiferromagnetic interaction in complex **1**. The magnetic data have been fitted considering complex **1** as a pseudo-dinuclear system, with the two copper(II) atoms bridged by two carboxylate oxygen atoms, since the coupling through long fum bridge is almost nil. The best-fit parameters obtained with this model are $J = -60$ cm^{-1}, $g_{Cu} = 2.20$.

Introduction

The design and synthesis of polynuclear metal complexes have become and active area of research for the last few decades due to their interesting molecular structure, crystal packing motifs and potential application in the field of magnetism,[1] fluorescence,[2] catalysis[3] and bio-inorganic chemistry.[4] The choice of ligands is one of the important factors for designing such polynuclear metal complexes. Chelating organic ligands block some coordination sites of the metals ions, whereas the organic spacers serve to link the metal ions and form polynuclear metal complexes.[5] Multidentate flexible Schiff bases are often used to build polynuclear complexes, since they can efficiently block some coordination sites of metal ions.[6] The use of Schiff base in combination with the linear dicarboxylate is an important strategy for synthesis of polynuclear complexes and in this combination the Schiff bases function as chelating ligand and linear dicarboxylate behaves as spacer.[7] Among the 3d metal ions the polynuclear chemistry of Cu(II) is very important since it exhibits a rich variety of coordination geometries e.g., tetragonal, tetrahedral, square planar, trigonal bipyramidal etc. and hence the prediction of final structure and molecular topology of

polynuclear copper (II) compounds is difficult.[8] On the other hand copper compounds show interesting magnetic properties,[9] anticancer activity[10] and bio-inorganic modeling.[11]

Fumaric acid (H$_2$fum), as a member of multidentate aliphatic dicarboxylic acids, possesses versatile coordination mode and have special conformation with a 180° angle between the carboxylic acid groups. It can function as mediator for transmitting the exchange interaction between the paramagnetic metal centers.[12] It has been scarcely used to construct the Cu(II) polynuclear complexes and to our knowledge only a few compounds of Cu(II) with fum^{2-} have been reported in the literature.[13] Since the metal-metal distance through the fum^{2-} ligand is above 9.2 Å, the bridging spacer does not effectively transmit magnetic exchange, however fum^{2-} sometimes function as monoatomic bridging mode and exhibit ferromagnetic exchange interaction.[13a]

Literature survey reveals that many copper(II) based coordination compounds are used as metallo-pharmaceuticals[14] and these compounds play an important role in biology due to their antimicrobial,[15] antifungal,[16] antibacterial,[17] antitumoral,[18] antiviral,[19] antipyretic[16a] and antidiabetic activities.[20] The study of the interaction of copper(II) compounds with DNA under physiological conditions is important for the design of copper(II) based new pharmaceuticals. On the other hand, serum albumin is the most abundant soluble protein in the circulatory system and function as transporter and disposer of pharmaceuticals.[21] For this reason the analysis of kinetics of the interaction of DNA / serum albumins and copper complex is important to determine the affinity of copper complex to DNA / protein, and this information will promote the development of copper metal based efficient metallopharmceuticals. In the present contribution we report synthesis, crystal structure and magnetic properties of a 1D polynuclear copper(II) compound, {[Cu$_2$(L)$_2$(fum)]·H$_2$O}$_n$ (**1**) (fum = fumarate ; HL = (E)-2-((1-hydroxybutan-2-

ylimino)methyl)phenol). Kinetics of interactions of complex **1** with calf thymus DNA (CT-DNA) and bovine / human serum albumins have been studied.

Experimental

Materials. High purity 2-amino-1-butanol was purchased from the Aldrich Chemical Co. Inc. and used as received. All other chemicals used were of analytical grade. Solvents used for spectroscopic studies were purifies and dried by standard procedures before use.[22]

Physical measurements. Elemental analyses (carbon, hydrogen and nitrogen) were performed using a Perkin-Elmer 240C elemental analyzer. IR spectra were recorded as KBr pellets on a Bruker Vector 22FT IR spectrophotometer operating from 400 to 4000 cm^{-1}. Electronic absorption spectra were obtained with Shimadzu UV-1601 UV-vis spectrophotometer at room temperature. Quartz cuvettes with a 1 cm path length and a 3 cm^3 volume were used for all measurements. Emission spectra were recorded on a Hitachi F-7000 spectrofluorimeter. Room temperature (300 K) spectra were obtained in methanolic solution using a quartz cell of 1 cm path length. The slit width was 2.5 nm for both excitation and emission.

The fluorescence quantum yield was determined using phenol as a reference and methanol medium for both complexes and reference. Emission spectra were recorded by exciting the complex and the reference phenol at the same wavelength, maintaining nearly equal absorbance (~ 0.1). The area of the emission spectrum was integrated using the software available in the instrument and the quantum yield calculated[23] according to the following equation:

$$\Phi_{\mathrm{s}} = \Phi_{\mathrm{r}} \frac{\mathrm{A_s}}{\mathrm{A_r}} \frac{\mathrm{I_r}}{\mathrm{I_s}} \frac{\eta_{\mathrm{s}}^2}{\eta_{\mathrm{r}}^2}$$

4

where Φ_s and Φ_r are the fluorescence quantum yield of the sample and reference, respectively. A_s and A_r are the respective optical densities at the wavelength of excitation, I_s and I_r correspond to the areas under the fluorescence curve; and η_s and η_r are the refractive index values for the sample and reference, respectively.

Temperature-dependent molar susceptibility measurements of polycrystalline sample was carried out at the *Servei de Magnetoquímica* of the *Centres Científics i Tecnològics* at the Universitat de Barcelona in a Quantum Design SQUID MPMSXL susceptometer with an applied field of 3000 and 198 G in the temperature ranges 2–300 and 2–30 K, respectively.

Synthesis of the ligands :

A methanolic solution (20 mL) of mixture of 2-amino-1-butanol (1 mmol, 0.089 g) and salicyldehyde (1 mmol, 0.122 g) was refluxed for 3h. The resulting yellow colour solution cooled to room temperature and solid yellow compound was obtained after evaporation of solvent under reduced pressure. The compound obtained was redissolved in MeOH and filtered. The solution was left for slow evaporation at room temperature. After one week, yellow crystals of HL were obtained. Yield: 85%. *Anal.*Calc. for $C_{11}H_{15}NO_2$ (193.24): C, 68.36; H, 7.82; N, 7.24 %. Found: C, 68.34; H, 7.79; N, 7.26 %. HR-MS: $[M + H]^+$, m/z, 194.25 (100%) calcd: m/z, 193.24. ^{1}H NMR (400 MHz, $CDCl_3$, δ ppm): 0.709-0.886 (3H, m), 1.474-1.655 (2H, m), 2.576 (1H, s), 3.466-3.690 (1H, m; 2H, m), 4.957 (1H, s), 6.823-6.921 (1H, d; 2H, m), 7.226-7.298 (1H, d; 2H, m), 8.306 (1H, s). ^{13}C NMR ($CDCl_3$, 400 MHz, δ ppm): 165.41 (Ar−C−OH), 161.71 (−CH=N−), 132.45-113.71 (Ar−C), 73.03 (-CH_2-OH), 66.23 (=N-CH-), 25.05 (-CH_2-), 10.51 (-CH_3).

Synthesis of complexes

Caution! Metal perchlorates in the presence of organic ligands are potentially explosive. Only a small amount of the material should be prepared and handled with care.

The complex has been synthesized by adopting the procedure schematically given in Scheme 1.

Scheme 1. Synthesis of complex **1**
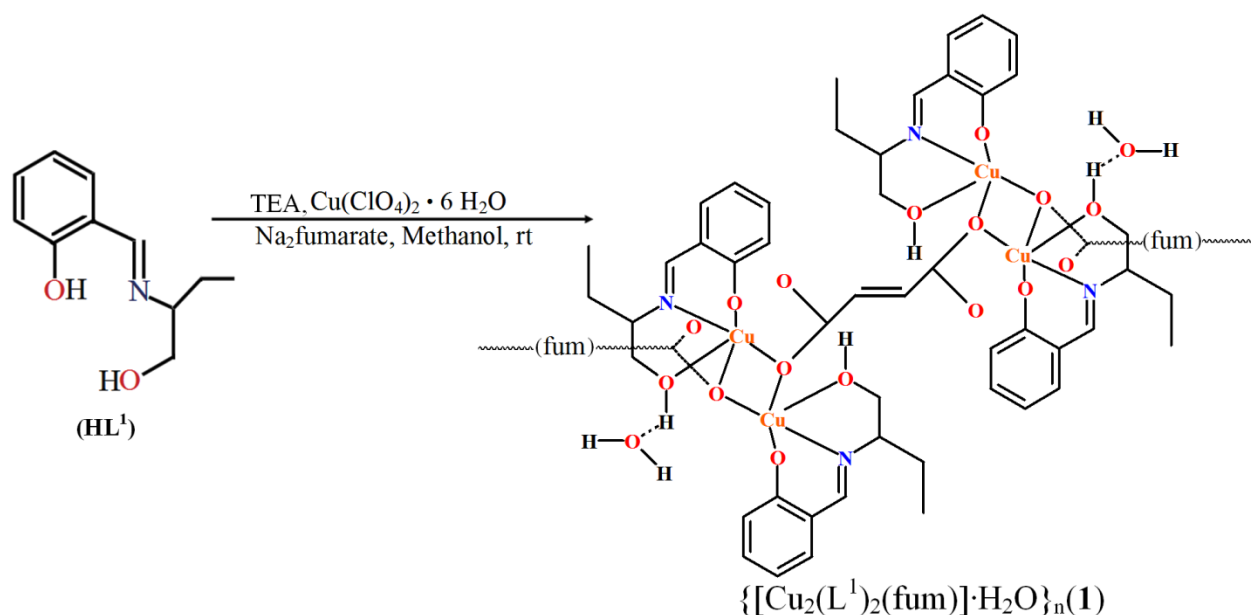
$$\{[Cu_2(L^1)_2(fum)]\cdot H_2O\}_n(\mathbf{1})$$

Synthesis of $\{[Cu_2(L)_2(fum)]\cdot H_2O\}_n$ (1). A methanolic solution (10 mL) of mixture of HL (1 mmol, 0.193 g) and triethylamine (TEA) (1 mmol) was added to a methanolic solution (10 mL) of $Cu(ClO_4)_2\cdot 6H_2O$ (1.0 mmol, 0.371 g), and stirred for 2h. To the resulting green mixture an aqueous solution (1 mL) of disodium fumarate (1mmol, 0.16 g) was added dropwise and resulting deep green reaction mixture was stirred for an additional 1 h at 27 °C and filtered. The filtrate was kept in air for slow evaporation at room temperature. Deep green needle shaped single crystals suitable for X-ray diffraction were obtained by slow evaporation of methanolic solution after a few days. Yield 78 %. *Anal.* Calc. for $C_{26}H_{32}Cu_2N_2O_9$ (643.62): C, 48.47; H, 4.97; N, 4.35 %. Found: C, 48.50; H, 4.99; N, 4.37 %. IR (cm^{-1}): 3200-3600 (br, vs), 2982 (w), 1642 (s), 1552 (vs), 1468 (s),

1416 (vs), 1374 (s), 1302 (vs), 1244 (vw), 1196 (vw), 1082 (vw), 1021 (vw), 888 (vw), 691 (br, vw).

Crystallographic data collection and refinement.

The crystal data of complex **1** was collected at room temperature using a Nonius Kappa CCD diffractometer with graphite monochromated Mo-Kα radiation. The data set was integrated with the Denzo-SMN package[24] and corrected for Lorentz, polarization and absorption effects (SORTAV).[25] The structure was solved by direct methods using SIR97[26] system of programs. The structure of **1** was refined using full-matrix least-squares with all non-hydrogen atoms anisotropically and hydrogens included on calculated positions, riding on their carrier atoms, except the hydrogen atoms forming H-bonds which were refined isotropically. The methyl group $C26\text{-}H_3$ was found disordered and refined isotropically over two positions with occupancies of 0.6 and 0.4, respectively. The structure displays large voids occupied by disordered solvent molecules which cannot be localized. These solvent molecules have been treated as a diffuse contribution to the overall scattering without specific atom positions using the routine SQUEEZE included in the PLATON systems of programs.[27] All calculations were performed using SHELXL-97[28] and PARST[29] implemented in WINGX[30] system of programs. Crystallographic data has been deposited at the Cambridge Crystallographic Data Centre and allocated the deposition numbers CCDC 1476311. The crystal data are given in Table 1 and a selection of bond distance and angles are given in Table 2.

Albumin Binding studies

Stock solutions of human serum albumin (HAS, 3.109 µM) and bovine serum albumin (BSA, 8.214 µM) were prepared in HEPES buffer (pH 7.2) solution. Aqueous solution of the copper(II) compound was prepared by dissolving the compound in water : HEPES buffer (1:99). The

interactions of compound with serum albumins were studied by recording room temperature tryptophan fluorescence of HSA / BSA at 340 nm. Fluorescence spectra were recorded in the range 290-450 nm at an excitation wavelength of 280 nm. To the solutions of serum albumins, copper(II) compound was added and the quenching of emission intensities at 340 nm (λ_{ex}, 280 nm) were recorded after gradual addition (20 µL, 0.199 µM) aqueous solution compound. The Stern-Volmer constant (K_{sv}) and quenching rate constant (k_q) were calculated using the equations $F_0/F = 1 + K_{sv}[complex]$ and $K_{sv} = k_q\tau_0$, where F_0 and F are the fluorescence intensity in the absence and in the presence of the complex, and τ_0 is the lifetime of serum albumin ($\sim 5 \times 10^{-9}$ s).[31] To calculate the binding constant of the compound with SA, the following Scatchard equation have been used

$\log[(F_o–F)/F] = \log K_b + n \log[complex]$, where K_b is the binding constant of the compound with serum albumin and n is the number of binding sites per albumin.

DNA binding studies

Absorbance spectral studies

UV spectroscopic technique has been used to investigate the possible binding mode and to calculate the intrinsic binding constant (K_{ib}) for the interaction of the complex with CT-DNA. Electronic absorption spectral titration was carried out at a fixed concentration of copper(II) compound (11.26 µM) in water and varying the concentration of CT-DNA from 0 to 23.21 µM. Intrinsic binding constant (K_{ib}) of the complex with CT-DNA was determined using the equation[32]

$$\frac{[DNA]}{(\varepsilon_a - \varepsilon_f)} = \frac{[DNA]}{(\varepsilon_b - \varepsilon_f)} + \frac{1}{K_{ib}(\varepsilon_b - \varepsilon_f)}$$

where, [DNA] is the concentration of CT-DNA, ε_a is the extinction co-efficient of the complex at a given CT-DNA concentration, ε_f and ε_b are the extinction co-efficient of the complex, in free solution and when fully bound to CT-DNA, respectively. The plot of $[DNA]/(\varepsilon_a-\varepsilon_f)$ *vs* [DNA] give

a straight line with $1/(\varepsilon_b-\varepsilon_f)$ and $1/[K_{ib}(\varepsilon_b-\varepsilon_f)]$ as slope and intercept, respectively. From the ratio of the slope to the intercept the value of K_{ib} was calculated.

Competitive binding fluorescence measurement

The competitive binding nature of ethidium bromide (EB) and copper(II) compound with CT-DNA was investigated adopting fluorometric method using aqueous solution of EB bound CT-DNA in HEPES buffer (pH 7.2) at room temperature. In presence of DNA, ethidium bromide (EB) exhibits fluorescence enhancement due to its intercalative binding to DNA. Competitive binding of copper(II) compound with CT-DNA results fluorescence quenching due to displacement of EB from CT-DNA. The fluorescence intensities at 612 nm (λ_{ex}, 500 nm) of EB bounded CT-DNA with increasing concentration of copper(II) compound was recorded. The Stern-Volmer constant (K_{sv}) was calculated using Stern-Volmer equation[33] $F_0/F = 1 + K_{sv}[complex]$,where F_0 and F are the emission intensity in absence and in presence of copper(II) compound, K_{sv} is the Stern-Volmer constant, and [complex] is the concentration of copper (II) compound.

Results and discussion

Crystal structure description

Complex **1** crystallizes in the monoclinic system with space group P21/n. Crystallographic data and selected bend lengths and bond angles are depicted in Table 1 and Table 2. The ORTEP[34] view of the asymmetric unit is shown in Fig.2 and the polymeric structure is shown in Fig.3. The crystal structure analysis complex **1** shows that the $Cu_2(L^1)_2$ units are connected by fumarate spacer, beside the presence of lattice water molecules. The crystallographic independent unit contains two copper(II) cation, two deprotonated Schiff base $(L^1)^-$, one fumarate and one lattice water molecule. Copper atoms of asymmetric unit are again connected with fumarate and form ID coordination polymeric structure (Fig.3). The coordination polyhedron for each metal is best described as

9

slightly distorted square pyramidal geometry [trigonality τ_5 parameters[35] are 0.128 and 0.013 for Cu(1) and Cu(2), respectively]. The basal plane is occupied by the chelating tridentate Schiff base donors [O(1), N(1), O(2) for Cu(1) and O(7), O(8), N(2), for Cu(2)] and by the fumarate oxygen donors [O(3) and O(5) for Cu(1) and Cu(2), respectively]. The apex of the square pyramid occupied by another fumarate oxygen at relatively longer distance [Cu(1)-O(5)' 2.384(5) Å; Cu(2)-O(3)" 2.476(4) Å (Table 2)]. The copper atoms are displaced by 0.0363 and 0.013 Å for Cu(1) and Cu(2), respectively, from the respective basal planes. The coordination Cu-O bond distances are varying in the range 1.908 - 2.384 Å and 1.909 - 2.476 Å for Cu(1) and Cu(2), respectively. The cisoid bond angle ranges are 78.46 - 94.95° for Cu(1) and 76.25 - 94.48° Cu(2) center. On the other hand the transoid bond angles are 166.88°, 174.56° (for Cu(1)), and 175.30°, 176.13 ° (for Cu(2)). The packing diagram of complex **1** indicates that it exists as 1D polymeric chain through fumarate linkage where Cu…Cu separation is 8.99Å. A weak coordinative interaction between Cu(1) and O(4) atoms [Cu(1)-O(4) 2.768 Å] also exists in the 1D chain. The 1D polymeric chains are involve in strong π…π interactions (Fig.1S) (centroid to centroid distance 3.66 Å, Table 1S) and results 2D supramolecular sheets. Two such different 2D sheets   are further connected with C–H…π interactions[36] (C–H…π (ring), 3.004 Å) and form a 3D supramolecular network (Fig.4).

IR, electronic absorption and fluorescence spectra of 1

IR spectrum of complex **1** is shown in Fig. 2S, and the most important absorption bands are summarized in the experimental section. The spectrum of complex **1** shows broad band in the region 3100 - 3600 cm^{-1} corresponding to the ν(O-H) stretching vibrations[37]. The band at 2982 cm^{-1} is due to the ν(C-H) stretching vibration. The asymmetric and symmetric stretching vibrations of carboxylate group appear at 1642 and 1416 cm^{-1}, respectively. The strong and sharp band at 1552 cm^{-1} is due to the aliphatic ν (C=N) stretching vibration.

The electronic spectrum of complex **1** shows (Fig. 5) significant transitions at 222 ($\varepsilon \sim 4.98 \times 10^4$ $M^{-1} cm^{-1}$), 238 ($\varepsilon \sim 4.40 \times 10^4 M^{-1} cm^{-1}$), 268 ($\varepsilon \sim 2.72 \times 10^4 M^{-1} cm^{-1}$) and 366 ($\varepsilon \sim 1.03 \times 10^4 M^{-1} cm^{-1}$) nm. Study of the luminescence property (Fig.5) of complex **1** shows red shifted emission (Table 3) with large Stokes shifts (44 - 96 nm). On excitation at 366 nm complex **1** exhibits emission at 410, 433 and 462 nm in methanol with a fluorescence quantum yield $\varphi = 0.257$, at room temperature. This band positions remain unchanged when λ_{ex} varied between 356 and 376 nm.

Protein binding studies

Serum albumin binding study using absorption spectroscopy

The change of electronic absorption spectra of bovine serum albumin (BSA) (3 ml, 8.214 µM aqueous solution) and human serum albumin (HSA) (3 ml, 3.109 µM aqueous solution) in presence of different concentration (0 - 14.748 µM) of complex **1** (using HEPES buffer, pH 7.2) at 300 K temperature is shown in Fig. 6. Spectral band at 280 nm of both serum albumins blue shifted in presence of complex **1** (6 nm for BSA, 7 nm for HAS at 27 °C; 7 nm for BSA, 8 nm for HAS at 37 °C). Bathochromic shift at 280 nm confirms the ground state association of complex **1** with serum albumins. The apparent association constants (K_{app}) were calculated adopting the following equation

$$\frac{1}{(A_{obs} - A_0)} = \frac{1}{(A_c - A_0)} + \frac{1}{K_{app}(A_c - A_0)[complex]}$$

where A_{obs} is the observed absorbance at 280 nm of the solution containing different concentrations of the complex, A_0 is the absorbance of serum albumin only and A_c is the absorbance of serum albumin with complex **1**. From the plot (Fig.7) of $1/(A_{obs}-A_0)$ *vs* $1/[complex]$ the values of apparent association constants were calculated and the calculated values are 1.34×10^4 L mol^{-1} and 1.81×10^4 L mol^{-1} for BSA and HAS, respectively, at 300 K (Table 4).

Fluorescence quenching of serum albumins by complex 1

The binding interactions of serum albumins with the complex were studied by fluorescence spectroscopy. On excitation at 280 nm, aqueous solution (pH 7.2, HEPES buffer) of serum albumins (BSA/HAS) exhibit luminescence at 340 nm. The change of fluorescence spectra of BSA and HAS upon addition of increasing concentration (0 - 11.269 µM) of complex 1 are shown in Fig.8. Significant decrease in fluorescence intensity (up to 68.67 % with 3 nm blue shift for BSA and up to 63.19 % with 2 nm blue shift for HAS) observed at 340 nm upon gradual addition of 20 µL, 0.199 µM aqueous solution of complex **1** to the solution of serum albumins. This hypochromicity in the spectra reveals that complex binds with serum albumins. From the Stern-Volmer equation[33] a linear relationship were obtained (R = 0.988 for BSA curve; R = 0.994 for HSA curve) for the titration of serum albumins using complex **1** as quencher (Fig. 8, inset). The calculated values of Stern-Volmer quenching constants (K_{sv}) are 2.09×10^5 L mol^{-1} (for BSA) and 1.39×10^5 L mol^{-1} (for HSA). Calculated values of the quenching constants (k_q) are 4.18×10^{13} L mol^{-1} s^{-1} and 2.79×10^{13} L mol^{-1} s^{-1} for BSA and HAS, respectively (Table 4). The values of K_{sv} and k_q indicate that complex **1** has good fluorescence quenching ability. The UV-vis absorption spectra of BSA/HAS show significant change on addition of complex **1**, this phenomenon indicate the existence of static interaction between BSA/HSA and complex **1**. The presence of static interaction is again supported by the very high values of k_q (~ 10^{13} L mol^{-1} s^{-1}), these are much greater than the maximum values (2×10^{10} L mol^{-1} s^{-1}) of diffusion collision quenching rate constant of various kind of fluorescence quenchers for biopolymer.[38] The binding constants (K_b) for the interaction of serum albumins with complex **1** and the number of binding sites (n) per albumin were also calculated using Scatchard equation. The plot of $\log \frac{(F_o - F)}{F}$ *vs* log[complex]

12

gives a straight line (Fig.9) with n and $\log K_b$ as slope and the intercept, respectively. Calculated values of k_b and n are given in Table 4.

DNA binding studies of complex

Electronic absorption spectral titration

The intercalation between a compound and DNA[39] is evident by the hypochromism in the electronic spectra of compound with or without red / blue shift upon gradual increasing concentration of DNA. On the contrary non-intercalative interaction between the compound and DNA supported by the hyperchromism in the absorption spectra of a compound with increasing concentration of DNA.[40] Fig.10 displays the change in the electronic absorption spectra of complex **1** (0.199 μM aqueous solution) with increasing concentration of CT-DNA (0 - 20.94 μM). The hypochromism of about 48.14, 25.14, and 25.18 % were observed for the spectral bands at 238, 268, and 366 nm, respectively. The bands at 238 and 268 nm showed hypochromism with 2 nm red shift and 1 nm blue shift, respectively, where no shifting observed for 366 nm band. These spectral changes indicate that complex **1** bind to the CT-DNA helix via intercalation. $[DNA]/(\varepsilon_a - \varepsilon_f)$ vs [DNA] (Fig. 10, inset) is a straight line with $\frac{1}{(\varepsilon_b - \varepsilon_f)}$ and $\frac{1}{K_{ib}(\varepsilon_b - \varepsilon_f)}$ as slope and intercept, respectively. The values of intrinsic binding constant (K_{ib}) was calculated from the ratio of slope to the intercept and calculated value of K_{ib} is 2.96×10^5 L mol^{-1}.

Ethidium Bromide (EtBr) displacement studies

Ethidium bromide (EtBr = 3,8-diamino-5-ethyl-6-phenyl phenanthridinium bromide) shows fluorescence with an orange colour, when it exposed to ultra violet radiation. The intensity of EtBr fluorescence increases around 20 fold in presence of CT-DNA due to strong intercalation of the

planar ethidium bromide phenanthridium ring between adjacent base pair of the double helix.[41] CT-DNA bounded EtBr shows emission at 612 nm on excitation at 500 nm. Addition of a compound, which is capable to interact with CT-DNA, to the solution of a mixture of EtBr-CT-DNA results in the quenching of EtBr-CT-DNA fluorescence intensity. The quenching of fluorescence occurs due to decrease in the number of binding sites on the CT-DNA available for EtBr. The fluorescence quenching observed in presence of compound may be used to study intercalation between CT-DNA and this compound. Fig.11 shows the change of fluorescence spectra of CT-DNA bounded EtBr upon gradual addition of 20 µL 0.199 µM solution of complex **1**. Hypochromism (up to 65.58 % of the initial fluorescence intensity of 612 nm band) in presence of complex **1** suggests that it displaced EtBr molecule from the DNA binding sites.[41, 42] From the Stern-Volmer plot[33] (insets of Fig. 11) the binding constant (K_{sv}) was calculated and it is 1.701×10^5 L mol^{-1}.

Magnetic properties of complex 1

Temperature-dependent magnetic susceptibility measurements on a polycrystalline sample of complex **1** were carried out in the temperature range 1.9-300 K. The plot of $\chi_M T$ versus T is shown in Fig. 12, where χ_M is the molar magnetic susceptibility and T is the absolute temperature. The $\chi_M T$ value measured at room temperature of 0.84 cm^3 K mol^{-1} is slightly higher than the expected value for two uncoupled S = ½ spins assuming g = 2 (0.75 cm^3 K mol^{-1}). Upon cooling, $\chi_M T$ varies smoothly and finally drops to zero, reaching a plateau at temperatures below 10 K. The behavior displayed by complex **1** confirms the presence of an overall antiferromagnetic interaction in the complex. The experimental magnetic data were simulated with the MAGPACK program.[43] The model assumed the crystallographic equivalence of the two Cu(II) ions within the dinuclear unit by assigning one single g value for both ions. Additionally, the interaction between Cu$_2$ units

through the fumarate bridge was considered negligible, since it is expected to be between one and two orders of magnitude weaker than the interaction with in the Cu_2 dinuclear unit.[44] For the spin Hamiltonian $H = -JS_1S_2$, $S_1 = S_2 = S_{Cu}$, a good agreement between the experimental and simulated curves for **1** was found by using the following parameters: $g_{Cu} = 2.20$ and $J_{Cu-Cu} = -60$ cm^{-1}. Temperature-independent paramagnetism (TIP) was considered equal to 150×10^{-6} cm^{3}mol^{-1}. The simulated curve is represented together with the experimental values in Fig.12.

The antiferromagnetic coupling in complex **1** can be understood in the light of orbital symmetry considerations. The two copper(II) ions in the asymmetric unit are penta-coordinated and the two square pyramids formed are sharing one base-to-apex edge with parallel basal planes.[45] The unpaired electron in each Cu(II) ion resides mainly in the basal $d_{x^2-y^2}$ orbital. Thus, the two parallel magnetic orbitals are orthogonally connected through an axial position occupied by the monodentate fumarate bridge. If a perfect square-pyramid environment ($\tau = 0$) is assumed for both Cu(II) ions, there would be no overlap between their magnetic orbitals, and consequently the magnetic interaction would be negligible or weakly ferromagnetic. However, in complex **1** only Cu2 shows a local geometry close to that of a perfect square-pyramid ($\tau = 0.013$), while Cu1 exhibits a larger distortion ($\tau = 0.128$). Such distortion is responsible for an increase of the overlap between $d_{x^2-y^2}$ magnetic orbitals in the asymmetric unit, and as a result a moderate antiferromagnetic exchange operates between the two Cu(II) ions.[46]

Conclusion

In summary, we have presented here the synthesis, crystal structure, low-temperature magnetic behavior and study of the interactions with BSA/HAS and CT-DNA of a novel fumerate (fum) bridged complex of copper(II) using O,N,O donor chelating ligand. Copper(II)-Schiff base in

combination with linear rigid carboxylate fum generates a 1D polymeric chain. 3D supramolecular architecture of compound realized through $\pi\ldots\pi$ and C–H$\ldots\pi$ interactions. The CT-DNA and protein binding of the copper(II) complex was investigated using electronic absorption and fluorescence spectroscopic techniques. The compound binds effectively to CT-DNA through intercalation and the calculated value of intrinsic binding constant was 2.96×10^5 L mol^{-1}. Fluorescence spectroscopic study shows that interaction of complex with serum albumins occurs through ground state association process and the calculated value of the quenching constants are in the order of 10^{13} L mol^{-1} s^{-1}. Low temperature magnetic measurement reveals existence of antiferromagnetic interaction in this compound. Experimental magnetic data of the compound were fitted with a pseudo-dinuclear copper (II) model where the two paramagnetic ions are bridged by two carboxylate groups and assuming that the coupling through long bridging fum is almost nil.

Supplementary information

Tables for $\pi\ldots\pi$ and H-bonding interactions, Figures of IR spectrum, crystal structure and BSA/HSA interaction deposited as supplementary information

.

References

(1) a) D. Gatteschi and R. Sessoli, *Angew. Chem.*, 2003, **115**, 278-309; (b) R. E. P. Winpenny, *Adv. Inorg. Chem.*, 2001, **52**, 1-111; c) S. Petit, P. Neugebauer, G. Pilet, G. Chastanet, A.-L. Barra, A. B. Antunes, W. Wernsdorfer and D. Luneau, *Inorg. Chem.*, 2012, **51**, 6645-6654; d) S. C. Manna, E. Zangrando, A. Bencini, C. Benelli and N. Ray Chaudhuri, *Inorg. Chem.* 2006, **45**, 9114-9122.

(2) (a) B. Gole, A.K. Bar and P.S. Mukherjee, *Chem. Commun.* 2011, **47**, 12137-12139; (b) Z. Zhang, S. Xiang, X. Rao, Q. Zheng, F.R. Fronczek, G. Qian and B. Chen, *Chem. Commun.*, 2010, **46**, 7205-7207; (c) C. Zhang, Y. Che, Z. Zhang, X. Yang and L. Zang, *Chem. Commun.*, 2011, **47**, 2336-2338; (d) S. Pramanick, C. Zheng, X. Zhang, T.J. Emge and J. Li, *J. Am. Chem. Soc.*, 2011, **133**, 4153-4155; (e) S. Mistri, E. Zangrando and S. C. Manna, *Polyhedron*, 2013, **49**, 252-258.

(3) (a) A. Biswas, L. Kanta Das, M. G. B. Drew, C. Diaz and A. Ghosh, *Inorg. Chem.*, 2012, **51**, 10111-10121; (b) N. S. McCool, D. M. Robinson, J. E. Sheats and G. C. Dismukes, *J. Am. Chem. Soc.*, 2011, **133**, 11446-11449; (c) H. Seino and M. Hidai, *Chem. Sci.*, 2011, **2**, 847-857; (d) S. Thakurta, P. Roy, R. J. Butcher, M. S. El Fallah, J. Tercero, E. Garriba and S. Mitra, *Eur. J. Inorg. Chem.*, 2009, 4385-4395; (e) T. A. Fernandes, C. I. M. Santos, V. André, J. Kłak, M. V. Kirillova and A. M. Kirillov, *Inorg. Chem.*, 2016, **55**, 125-135; (f) S. Hazra, A. Karmakar, M. de Fátima C. G. da Silva, L'. Dlháň, R. Boča and A. J. L. Pombeiro, *New J.Chem.,* 2015, **39**, 3424-3434.

(4) (a) S. Vaddypally, S. K. Kondaveeti and M. J. Zdilla, *Inorg. Chem.*, 2012, **51**, 3950-3952; (b) C. R. Sharp, J. S. Duncan and S. C. Lee, *Inorg. Chem.*, 2010, **49**, 6697-6705; (b) R. H. Holm, P. Kennepohl and E. I. Solomon, *Chem. Rev.*, 1996, **96**, 2239-2314; (c) W. Kaim and B. Schwerderski, Bioinorganic Chemistry: Inorganic Elements in the Chemistry of Life, John Wiley, Chichester, 1994.

(5) S. C. Manna, E. Zangrando, J. Ribas and N. Ray Chaudhuri, *Eur. J. Inorg. Chem.* 2007, 4592-4595; (b) A. K. Ghosh, D. Ghoshal, E. Zangrando, J. Ribas and N. Ray Chaudhuri, *Inorg. Chem.* 2007, **46**, 3057-3071; (c) A. K. Ghosh, D. Ghoshal, E. Zangrando, J. Ribas and N. Ray Chaudhuri, *Dalton Trans.*, 2006, 1554-1563; (d) D. Ghoshal, T. K. Maji, G. Mostafa, S. Sain, T.-H. Lu, J. Ribas, E. Zangrando and N. Ray Chaudhuri, *Dalton Trans.*, 2004, 1687-1695.

(6) S. C. Manna, S. Konar, E. Zangrando, M. G. B. Drew, J. Ribas and N. Ray Chaudhuri, *Eur. J. Inorg. Chem.* 2005, 1751-1758; (b) P. S. Mukherjee, S. Dalai, G. Mostafa, T.-H. Lu, E.Rentschler and N. Ray Chaudhuri, *New J. Chem.*, 2001, **25**, 1203-1207.

(7) S. Choubey, S. Roy, K. Bhar, R. Ghosh, P. Mitra, C.-H. Lin, J. Ribas and B. K. Ghosh, *Polyhedron*, 2013, **55**, 1-9; (b) C. Chen, D. Huang, X. Zhang, F. Chen, H. Zhu, Q. Liu, C. Zhang, D. Liao, L. Li and L. Sun, *Inorg. Chem.* 2003, *42*, 3540-3548; (c) Y. Aono, H. Yoshida, K. Katoh, B. K. Breedlove, K. Kagesawa and M. Yamashita, *Inorg. Chem.*, 2015, **54**, 7096-7102.

(8) (a) M. Sutradhar, M. V. Kirillova, M. F.C. Guedes da Silva, C.-M. Liu and A. J. L. Pombeiro, *Dalton Trans.*, 2013, **42**, 16578-16587; (b) R. H. Bode, W. L. Driessen, F. B. Hulsbergen, J. Reedijk and A. L. Spek, *Eur. J. Inorg. Chem.*, 1999, 505-507; (c) M. Murugesu, R. Clerac, B. Pilawa, A. Mandel, C. E. Anson and A. K. Powell, *Inorg. Chim. Acta*, 2002, **337**, 328-336; (d) R. Acevedo-Chavez, M. E. Costas, S. Bernes, G. Medina and L. Gasque, *J. Chem. Soc., Dalton Trans.*, 2002, 2553-2558; (e) Z. Q. Xu, L. K. Thompson and D. O. Miller, *Chem. Commun.*, 2001, 1170-1171; (f) R. Ziessel, L. Charbonniere, M. Cesario, T. Prange and H. Nierengarten, *Angew. Chem., Int. Ed.*, 2002, **41**, 975-979; (g) B. Graham, M. T. W. Hearn, P. C. Junk, C. M. Kepert, F. E. Mabbs, B. Moubaraki, K. S. Murray and L. Spiccia, *Inorg. Chem.*, 2001, **40**, 1536-1543; (h) J. Sletten, A. Sørensen, M. Julve and Y. Journaux, *Inorg. Chem.*, 1990, **29**, 5054-5058.

(9) (a) S. Triki, J. S. Pala, M. Decoster, P. Molinié and L. Toupet, *Angew. Chem., Int. Ed.*, 1999, **38**, 113-115; (b) W. Plass, A. Pohlmann and J. Rautengarten, *Angew. Chem., Int. Ed.*, 2001, **40**, 4207-4210; (c) Y. S. You, J. H. Yoon, H. C. Kim and C. S. Hong, *Chem. Commun.*, 2005, 4116-4118; (d) S. Mukherjee, B. Gole, Y. Song and P. S. Mukherjee, *Inorg. Chem.*, 2011, **50**, 3621-3631; (e) S. Turba, S. P. Foxon, A. Beitat, F. W. Heinemann, K. Petukhov, P. Müller, O. Walter, F. Lloret, M. Julve and S. Schindler, *Inorg. Chem.*, 2012, **51**, 88-97; (f) C. Adhikarya and S. Koner, *Coord. Chem. Rev.*, 2010, **254**, 2933-2958; (g) D. Venegas-Yazigia, D. Aravenab, E. Spodineb, E. Ruizd and S. Alvarezd, *Coord. Chem. Rev.*, 2010, **254**, 2086-2095; (h) J. Mroziński, *Coord. Chem. Rev.*, 2005, **259**, 2534-2548.

(10) (a) B. Duff, V. R. Thangella, B. S. Creaven, M. Walsh and D. A. Egan, *Eur. J. Pharmacol.*, 2012, **689**, 45-55; (b) A. T. Chaviara, P. C. Christidis, A. Papageorgiou, E. Chrysogelou, D. J. Hadjipavlou-Litina and C. A. Bolos, *J. Inorg. Biochem.*, 2005, **99**, 2102-2109. (c) A. Bhunia, S. Manna, S. Mistri, A. Paul, R. K. Manne, M. K. Santra, V. Bertolasic and S. C. Manna, *RSC Adv.* 2015, **5**, 67727-67737; (d) S. Mistri, A. Paul, A. Bhunia, R. K. Manne, M. K. Santra, H. Puschmann and S. C. Manna, *Polyhedron*, 2016, **104**, 63-72; (e) M. Chen, X.-Y. Tang, S.-P. Yang, H.-H. Li, H.-Q. Zhao, Z.-H. Jiang, J.-X. Chen and W.-H. Chen, *Dalton Trans.*, 2015, **44**, 13369-13377.

(11) R. Than, A. A. Feldmann and B. Krebs, *Coord. Chem. Rev.*, 1999, **182**, 211-241.

(12) S. Konar, P. S. Mukherjee, E. Zangrando, F. Lloret and N. Ray Chaudhuri, *Angew. Chem, Int. Ed.,* 2002, **41**, 1561 - 1563; (b) S. C. Manna, E. Zangrando, J. Ribas and N. Ray Chaudhuri, *Dalton Trans.*, 2007, 1383-1391.

(13) (a) P. S. Mukherjee, T. K. Maji, G. Mostafa, J. Ribas, M. S. El Fallah and N. Ray Chaudhuri, *Inorg. Chem.* 2001, **40***, 928-931; (b) P. S. Mukherjee, D. Ghoshal, E. Zangrando, T. Mallah and N. Ray Chaudhuri, *Eur. J. Inorg. Chem.* 2004, 4675-4680.

(14) Y. Yoshikawa and H. Yasui, *Current Topics in Medicinal Chemistry*, 2012, **12**, 210-218.

(15) (a) M. S. Islas, J. J. M. Medina, L. L. L. Tévez, T. Rojo, L. Lezama, M. G. Merino, L. Calleros, M. A. Cortes, M. R. Puyol, G. A. Echeverría, O. E. Piro, E. G. Ferrer and P. A. M. Williams, *Inorg. Chem.,* 2014, **53**, 5724-5437; (b) A. Valent, M. Melnik, D. Hudecova, B. Dudova, R. Kivekas and M. R. Sundberg, *Inorg. Chim. Acta*, 2002, **340**, 15-20; (c) A. Wojciechowska, A. Gągor, W. Zierkiewicz, A. Jarząb, A. Dylong and M. Duczmal, *RSC Adv.*, 2015, **5**, 36295-36306.

(16) (a) A. M. Abu-Dief and I. M. A. Mohamed, *Beni-Suef university journal of basic and applied sciences,* 2015, **4**, 119-133; (b) F. Rahaman and B. H. M. Mruthyunjayaswamy, *Complex Met.*, 2014, **1**, 88-95.

(17) (a) S. Muche, I. Levacheva, O. Samsonova, L. Pham, G. Christou, U. Bakowsky and M. Hołyńska, *Inorg. Chem.*, 2014, **53**, 7642-7649.

(18) (a) D. -D. Yin, Y. -L. Jiang and L. Shan, *Chinese J. Chem.*, 2001, **19**, 1136-1140.

(19) (a) J. Vanˇco, O. ˇSvajlenova, E. Raˇcanska, J. Muselik and J. Valentova, *J. Trace Elem. Med. Biol.*, 2004, **18**, 155-161.

(20) J. Vančo, J. Marek, Z. Trávníček, E. Račanská, J. Muselík and O. Švajlenová, *J. Inorg. Biochem.*, 2008, **102**, 595-605.

(21) B. X. Huang, H. Y. Kim and C. Dass, J. Am. Soc. Mass Spectrom., 2004, **15**, 1237-1247.

(22) D. D. Perrin, W. L. F. Armarego, D. R. Perrin, Purification of Laboratory Chemicals; Pergamon Press: Oxford, U.K., 1980.

(23) J. R. Lakowicz, Principles of Fluorescence Spectroscopy, Third Edition, Springer, New York, USA, 2006.

(24) Z. Otwinowski, W. Minor, Methods in Enzymology, C.W. Carter, R.M. Sweet Editors, Part A, Academic Press, London, 1997, **276**, 307-326.

(25) R. H. Blessing, *Acta Crystallogr. Sect A,* 1995, **51**, 33-38.

(26) A. Altomare, M. C. Burla, M. Camalli, G. L. Cascarano, C. Giacovazzo, A. Guagliardi, A. G. Moliterni, G. Polidori and R. Spagna, *J. Appl. Crystallogr.* 1999, **32**, 115-119.

(27) A. L. Spek, *Acta Crystallogr.* 2009, **D65**, 148-155.

(28) G. M. Sheldrick, SHELX-97, Program for Crystal Structure Refinement, University of Gottingen, Germany, 1997.

(29) M. Nardelli, *J. Appl. Crystallogr.* 1995, **28**, 659-659.

(30) L. J. Farrugia, *J. Appl. Crystallogr.* 1999, **32**, 837-838.

(31) P. Smoleński, C. Pettinari, F. Marchetti, M. Fátima C. Guedes da Silva, G. Lupidi, G. V. B. Patzmay, D. Petrelli, L. A. Vitali, and A. J. L. Pombeiro, *Inorg. Chem.,* 2015, **54**, 434-440.

(32) A. Wolfe, G. H. Shimer and T. Mechan, *Biochemistry*, 1987, **26**, 6392-6396.

(33) J. R. Lakowicz, Principles of Fluorescence Spectroscopy, Third Edition, Springer, New York, USA, 2006.

(34) M. N. Burnett, C. K. Johnson, ORTEP III, Report ORNL-6895, Oak Ridge National Laboratory, Oak Ridge, TN, 1996.

(35) A. W. Addison, T. N. Rao, J. Reedijk, J. V. Rijn and G. C. Verschoor, *J. Chem. Soc. Dalton Trans.* 1984, 1349-1356.

(36) (a) M. Nishio, M. Hirota, Y. Umezawa, The C–H…π Interaction: Evidence, Nature and Consequences, Wiley-VCH, New York, 1998; (b) M. Nishio, *CrystEngComm,* 2004, **6**, 130-156;

(c) M. d. C. Fernandez- Alonso, F. J. Canada, J. Jimenez-Barbero and G. Cuevas, *J. Am. Chem. Soc.* 2005, **127**, 7379-7386; (d) D. Braga, S. L. Giaffreda, F. Grepioni, L. Maini and M. Polito, *Coord. Chem. Rev.* 2006, **250**, 1267-1285; (e) H. J. Schneider, *Angew. Chem., Int. Ed.* 2009, **48**, 3924-3977.

(37) K. Nakamoto, Infrared Spectra of Inorganic and Coordination Compounds; John Wiley & Sons: New York, 1997.

(38) (a) P. Smoleński, C. Pettinari, F. Marchetti, M. Fátima C. Guedes da Silva, G. Lupidi, G. V. B. Patzmay, D. Petrelli, L. A. Vitali, and A. J. L. Pombeiro, *Inorg. Chem.,* 2015, **54**, 434-440; (b) N. Shahabadi, M. M. Maghsudi and Z. Ahmadipour, *Spectrochim. Acta, Part A* 2012, **92**, 184-188; (c) J. Jing, M. Jiang, Y.- T. Li, Z.- Y. Wu and C.- W. Yan, *J. Biochem. Mol. Toxic.* 2014, **28**, 47-59; (d) L. Li, G. Q. Qiong, J. Dong, T. Xu and J. Li, *J. Photochem. Photobiol., B* 2013, **125**, 56-62; (e) S. Bi, B. Pang, T. Zhao, T. Wang, Y. Wang and L. Yan, *Spectrochim. Acta, Part A*, 2013, **111**, 182-187; (f) Y. Sun, H. Zhang, S. Bi, X. Zhou, L. Wang and Y. Yan, *J. Lumin.,* 2011, **131**, 2299-2306; (g) D. J. Li, J. F. Zhu and J. Jin, *J. Photochem. Photobiol., A,* 2007, **189**, 114-120; (h) W. R. Ware, *J. Phys. Chem.*, 1962, **66**, 455-458.

(39) (a) Q. -L. Zhang, J. -G. Liu, H. Chao, G. -Q. Xue and L. -N. Ji, *J. Inorg. Biochem.* 2001, **83**, 49-55; (b) Z. -C. Liu, B. -D. Wang, B. Li, Q. Wang, Z. -Y. Yang, T. -R. Li and Y. Li, *Eur. J. Med. Chem.* 2010, **45**, 5353-5361; (c) R. K. Gupta, G. Sharma, R. Pandey, A. Kumar, B. Koch, P.-Z. Li, Q. Xu, and D. S. Pandey, *Inorg. Chem.* 2013, **52**, 13984-13996.

(40) (a) F. Mancin, P. Scrimin, P. Tecilla and U. Tonellato, *Chem. Commun.* 2005, 2540-2548;(b) L. Tjioe, A. Meininger, T. Joshi, L. Spiccia and B. Graham, *Inorg. Chem.* 2011, **50**, 4327-4339.

(41) (a) P. Kumar, S. Gorai, M. Kumar, B. Mondal and D. Manna, *Dalton Trans.* 2012, **41**, 7573-7581; (b) K. Jeyalakshmi, Y. Arun, N. S. P. Bhuvanesh, P. T. Perumal, A. Sreekantha and R. Karvembu, *Inorg. Chem. Front.* 2015, **2**, 780-798.

(42) (a) J. -B. Lepecq and C. Paoletti, *J. Mol. Biol.* 1967, **27**, 87-93; (b) R. Palchaudhuri and P. J Hergenrother, *Current Opinion in Biotechnology,* 2007, **18**, 497-503; (c) A. J. Geall and I. S. Blagbrough, *J. Pharma. Biomed. Analysis,* 2000, **22**, 849-859; (d) M. A. Kostiainen, J. G. Hardy and D. K. Smith, *Angew. Chem. Int. ed.* 2005, **44**, 2556-2559.

(43) (a) J.J.Borràs-Almenar, J. M. Clemente-Juan, E. Coronado and B.S.Tsukerblat, J. *Comput. Chem.*, 2001, **22**, 985-991; (b) J.J.Borràs-Almenar, J. M. Clement-Juan, E. Coronado and B. S. Tsukerblat, *Inorg. Chem.*, 1999, **38**, 6081-6088.

(44) a) P. S. Mukherjee, S. Dalai, G. Mostafa, E. Zangrando, T.-H. Lu, G. Rogez, T. Mallah and N. R. Chaudhuri, *Chem. Comm.,* 2001, 1346-1347; b) P. S. Mukherjee, D. Ghoshal, E. Zangrando, T. Mallah and N. R. Chaudhuri, *Eur. J. Inorg. Chem.,* 2004, 4675-4680.

(45) M. Rodríguez, A. Llobet, M. Corbella, A. E. Martell and J. Reibenspies, *Inorg. Chem.* 1999, **38**, 2328-2334.

(46) V. K. Bhardwaj, N. Aliaga-Alcalde, M. Corbella and G. Hundal, *Inorg. Chim. Acta,* 2010, **363**, 97-106.

Table 1 Crystal Data and Structure Refinement for complex **1**

Empirical formula	$C_{26}H_{32}Cu_2N_2O_9$
Formula mass, g mol^{-1}	643.62
Crystal system	Monoclinic
Space group	P 21/n
a/Å	8.4944(3)
b/Å	13.2905(4)

c/Å	26.3919(9)
$\alpha/°$	90
$\beta/°$	96.916(1)
$\gamma/°$	90
U/Å^3	2957.8(2)
Z	4
T/K	295
D_c/g cm^{-3}	1.445
μ(Mo-Kα)/ cm^{-1}	14.89
F(000)	1328.0
θ_{min}- θ_{max}/°	3.07-25.50
Measured Reflections	15779
Unique Reflections	5472
R_{int}	0.0733
Obs. Refl.ns [I≥2σ(I)]	3525
hkl ranges	-10,10;-16,16;-25,31
Goodness of fit (F^2)	1.041
No. Variables/Restraints	379/5
R(F^2) (Obs.Refl.ns)	0.0709
wR(F^2) (All Refl.ns)	0.1754
$\Delta\rho_{max}$; $\Delta\rho_{min}$ /e Å^{-3}	0.615; -0.557

Table 2 Selected bond distances (Å) and angles (°) of complex **1**

Bond distances			
Cu(1)-O(1)	1.908(4)	Cu(2)-O(5)	1.944(4)
Cu(1)-O(2)	2.050(5)	Cu(2)-O(7)	1.909(4)
Cu(1)-O(3)	1.947(4)	Cu(2)-O(8)	1.995(4)
Cu(1)-N(1)	1.930(5)	Cu(2)-N(2)	1.938(5)
Cu(1)-O(5)'	2.384(5)	Cu(2)-O(3)"	2.476(4)
Bond angles			
O(1)-Cu(1)-O(2)	174.6(2)	O(7)-Cu(2)-O(8)	176.1(2)
O(1)-Cu(1)-O(3)	94.2(2)	O(7)-Cu(2)-O(5)	90.2(2)
O(1)-Cu(1)-N(1)	95.0(2)	O(7)-Cu(2)-N(2)	94.5(2)
O(1)-Cu(1)-O(5)'	94.5(2)	O(7)-Cu(2)-O(3)"	92.5(2)
O(2)-Cu(1)-O(3)	89.4(2)	O(8)-Cu(2)-O(5)	93.1(2)
O(2)-Cu(1)-N(1)	82.2(2)	O(8)-Cu(2)-N(2)	82.3(2)
O(2)-Cu(1)-O(5)'	82.1(2)	O(8)-Cu(2)-O(3)"	90.3(2)
O(3)-Cu(1)-N(1)	166.9(2)	O(5)-Cu(2)-N(2)	175.3(2)
O(3)-Cu(1)-O(5)'	78.5(2)	O(5)-Cu(1)-O(3)"	76.2(2)
N(1)-Cu(1)-O(5)'	110.1(2)	N(2)-Cu(1)-O(3)"	102.9(2)

Symmetry operations: (') at x+1,y,z and (") atx-1,y,z

Table 3 Photophysical parameters of complex **1**.

|	Absorption λ(nm), ε_{exp} ($M^{-1}cm^{-1}$)	Emission λ_{em} (nm)	Δv[a](nm)	φ
Complex **1**	222 (0.498×10^5), 238 (0.440×10^5), 268 (0.272×10^5), **366** (0.103×10^5)	410, 433, 462	44, 67, 96	0.257

Bold number indicates the excitation wavelengths. [a]Stoke shift

Table 4 Apparent binding constant (K_a), Stern-Volmer constant (K_{sv}), quenching constant (K_q), binding constant (K_b) and number of binding site (n) of BSA and HSA.

	K_a (L mol^{-1})	K_{sv} (L mol^{-1})	K_q(L mol^{-1}s^{-1})	K_b (L mol^{-1})	n
BSA	1.3468×10^4	2.0933×10^5	4.1866×10^{13}	7.8324×10^5	1.34
HSA	1.8153×10^4	1.397×10^5	2.794×10^{13}	7.5557×10^5	1.14

Table 5 DNA binding constant (K_b), quenching constant (K_q) and apparent binding constant (K_{app}) of complex **1**.

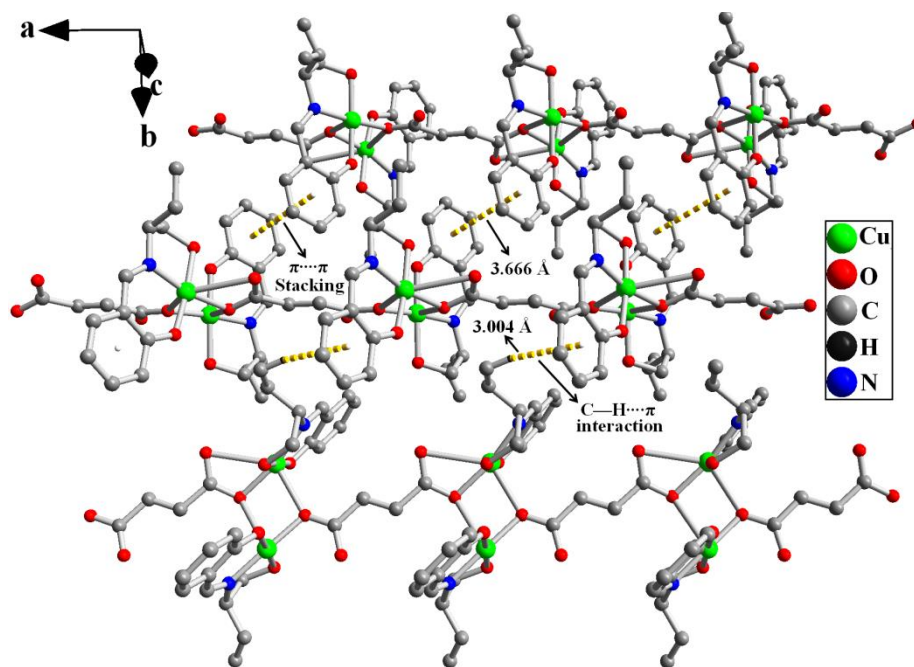| K_{ib} (M^{-1})	K_{sv}(M^{-1})	K_{app}(M^{-1})
2.961×10^5	1.7017×10^5	4.5437×10^6
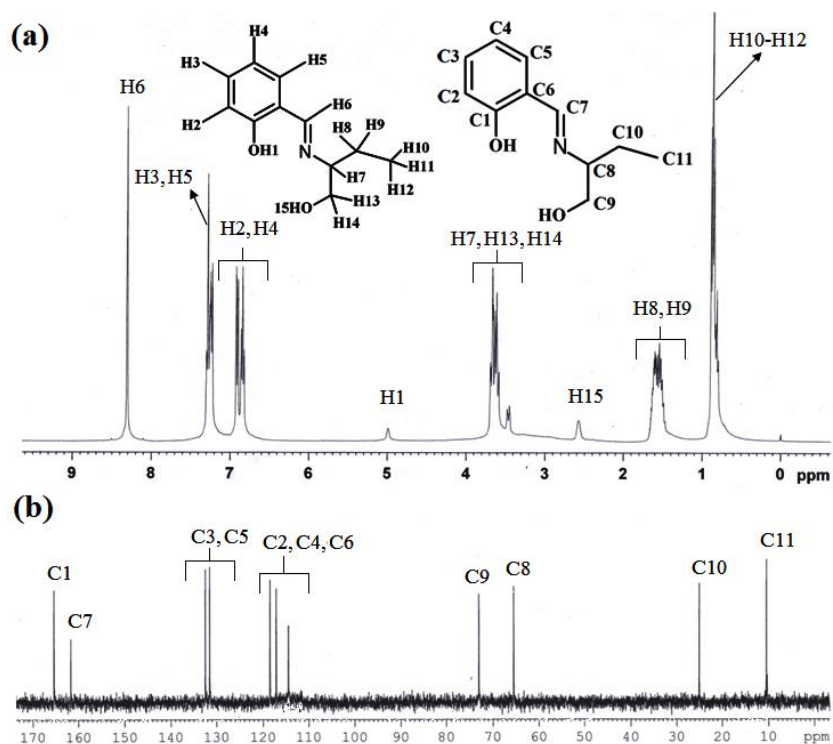
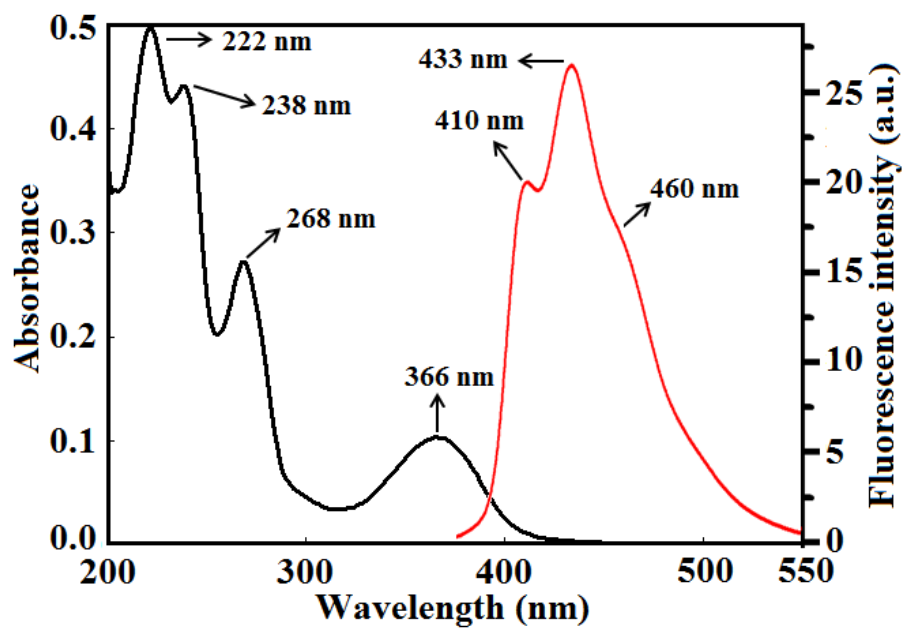**Fig. 1.** ^{1}H (**a**) and ^{13}C NMR (**b**) spectra of HL.
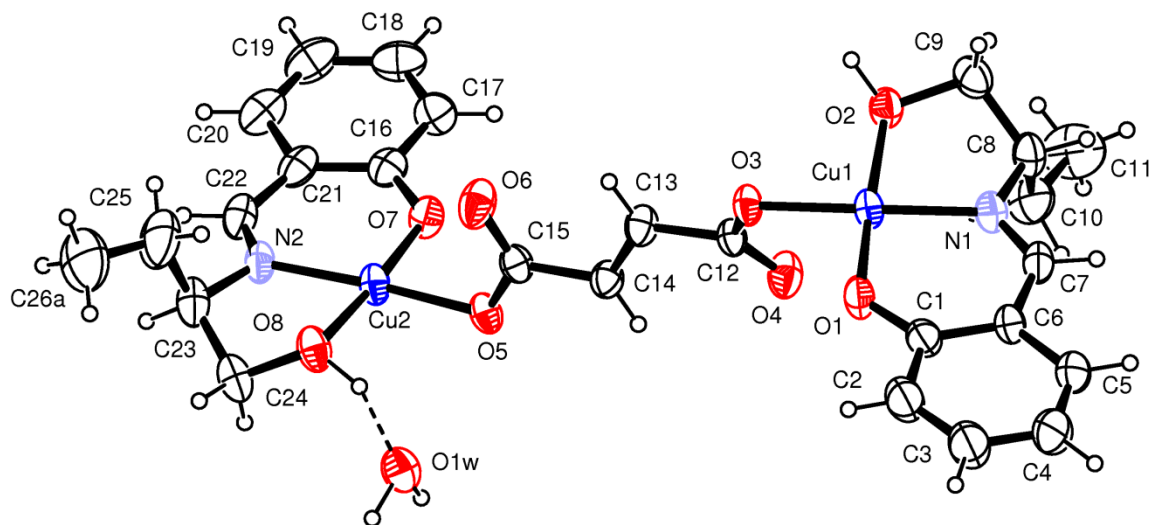
Fig.2. ORTEP view of the asymmetric unit of complex **1** showing the thermal ellipsoids at 30% probability level.
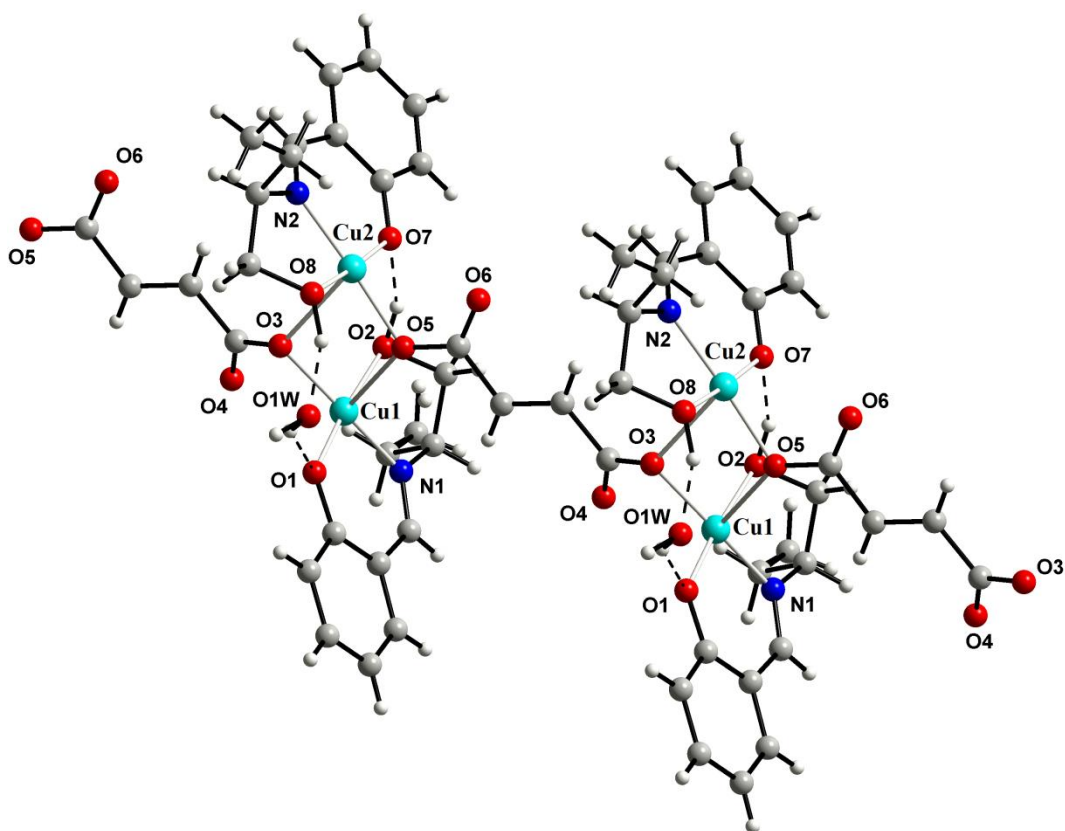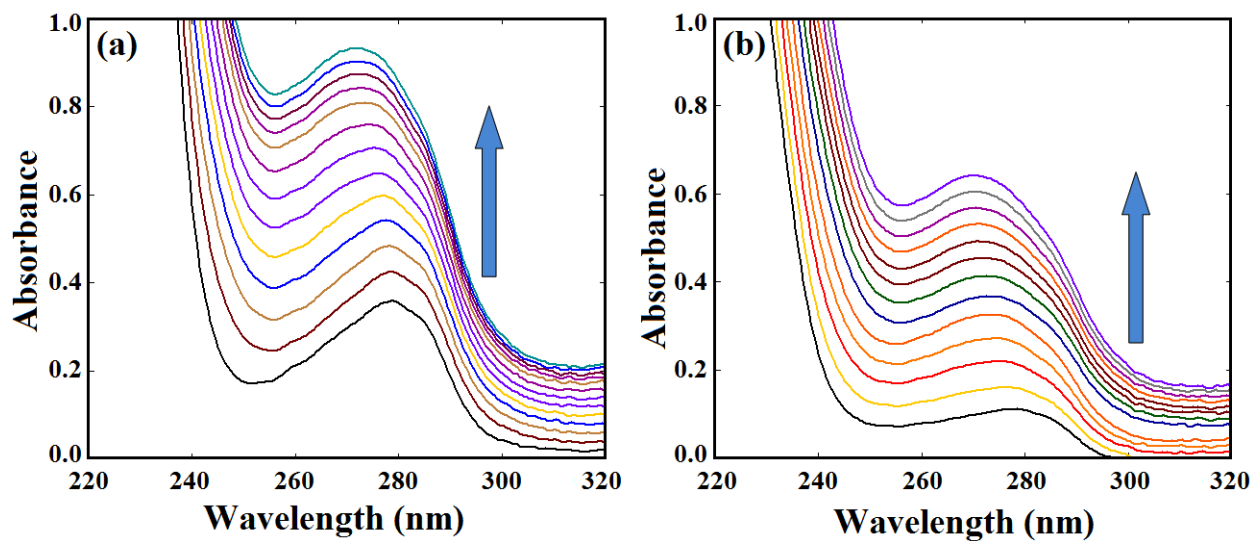
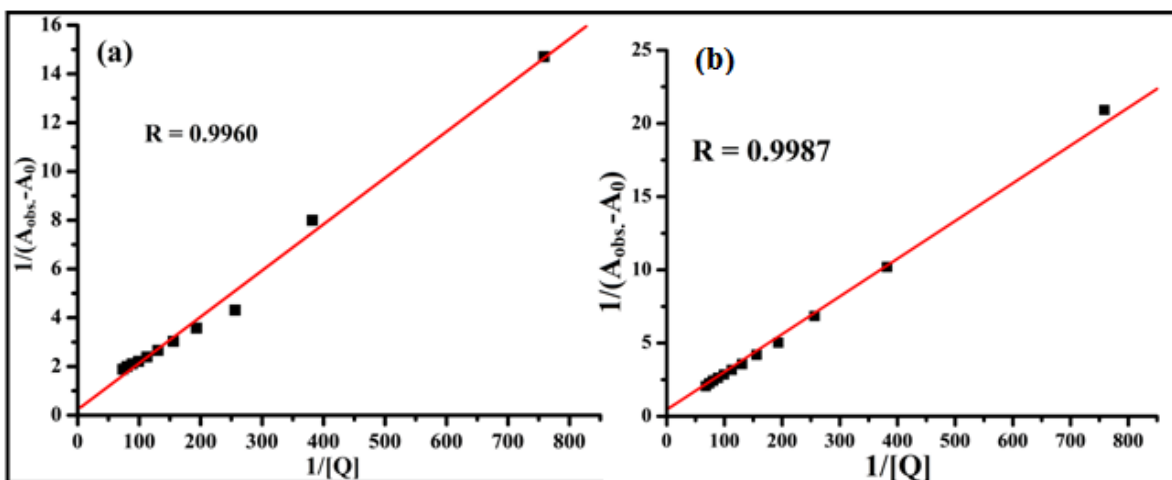**Fig.3.** The polymeric structure of complex **1** determined by the Cu1…O5 and Cu2…O3 interactions.

**Fig.4.** 3D supramolecular structure of complex **1** formed with π…π and C−H…π interactions.

**Fig. 5.** Electronic absorption and emission spectra of complex **1**.

Fig.6. Change of electronic absorption spectra of BSA (**a**) and HAS (**b**) upon gradual addition of complex **1** at temperature 300 K.
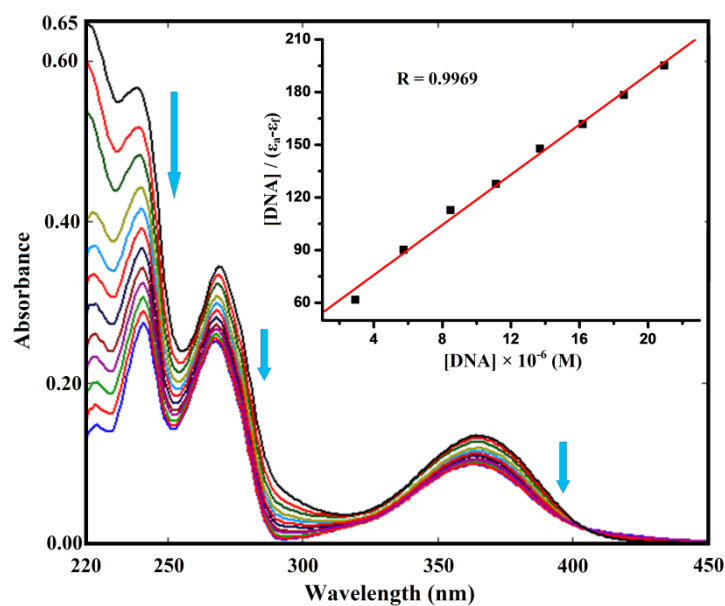
28

Fig.7. Plot of $1/(A_{obs.} - A_0)$ vs reciprocal of complex **1** concentration for titration with BSA (**a**) and HAS (**b**) at 300K.
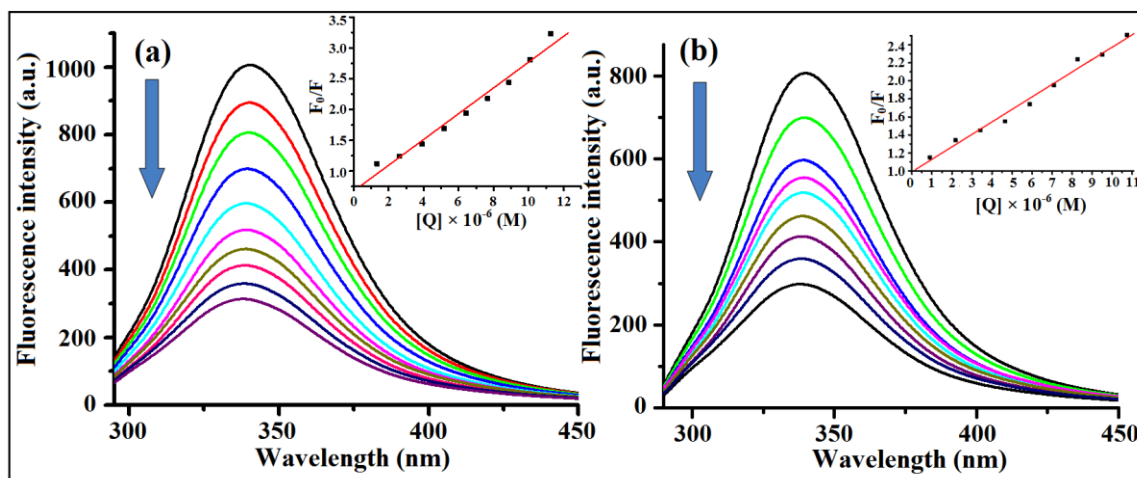

Fig.8. Titration of BSA (a) and HAS (b) with complex **1.** (Inset: Stern–Volmer plot for the titration).
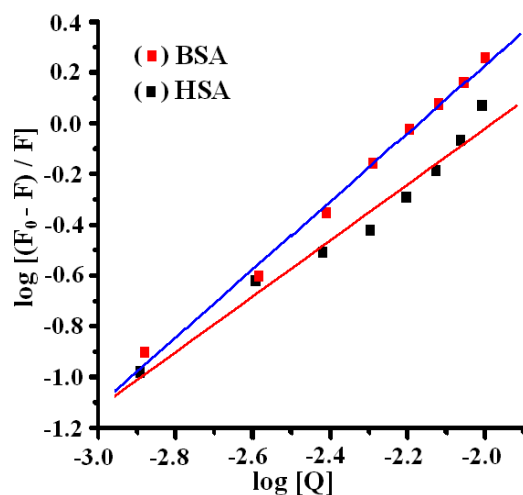
Fig.9. Double-logarithm curves of BSA and HSA fluorescence quenching by complex **1**

Fig.10. Electronic absorption spectra of complex **1** in the absence and presence of increasing amount of CT-DNA. Arrows show the changes in absorbance with respect to an increase in the DNA concentration. Inset: plot of [DNA]/ $(\varepsilon_a-\varepsilon_f)$ versus [DNA].
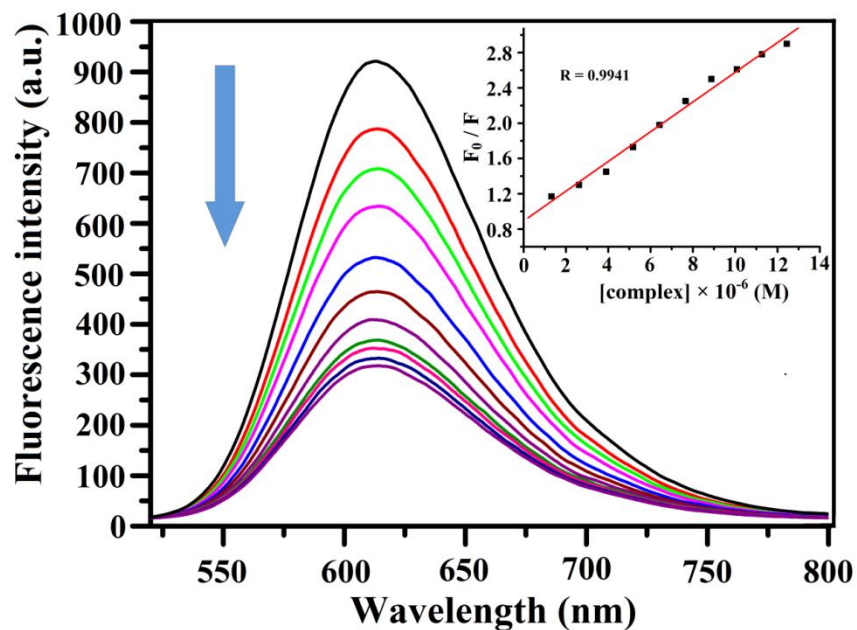
Fig.11. Emission spectra of EB-DNA in the presence of complex **1**. Arrow indicates the change in the emission intensity as a function of complex concentration. Inset: Stern-Volmer plot of the fluorescence titration data corresponding to the complex **1**.
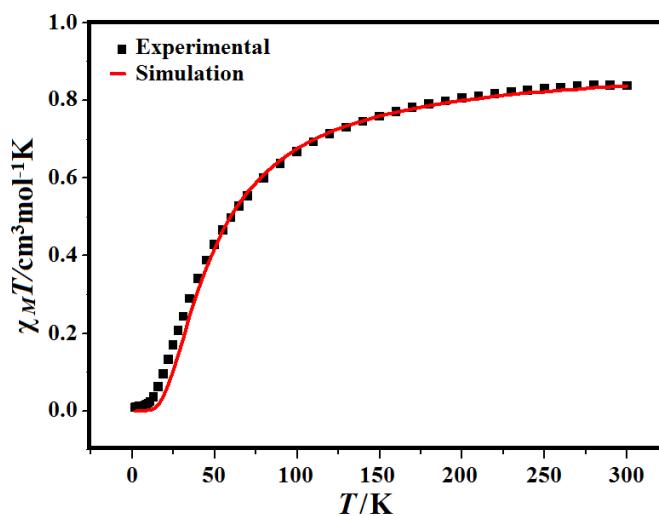
Fig.12. $\chi_M T$ vs. T plot for complex **1** (solid line represents the best fit).